Electronic Supplementary Material (ESI) for CrystEngComm.

Electronic Supporting Information

Nanostructured catalyst assembled from CNTs, $NiSe_2$ nanoparticles, and 2D Ni-MOF nanosheets for electrocatalytic hydrogen evolution reaction

Feng-Yuan Zhu,[‡a,b] Xiaoli Zhang,[‡a] Xu Han,[a] Chengyan Zhou,[a] Shuanglong Lu,*[c] Jian-Ping Lang*[a,b] and Hongwei Gu*[a]

[a] *College of Chemistry, Chemical Engineering and Materials Science, Soochow University, Suzhou, 215123, P. R. China. E-mail: jplang@suda.edu.cn, hongwei@suda.du.cn; Fax: 86-512-65883615*

[b] *State Key Laboratory of Organometallic Chemistry, Shanghai Institute of Organic Chemistry, Chinese Academy of Sciences, Shanghai 200032, P. R. China*

[c] *Key Laboratory of Synthetic and Biological Colloids, Ministry of Education, School of Chemical and Material Engineering, Jiangnan University, Wuxi 214122, Jiangsu, P. R. China. E-mail: lushuanglong@jiangnan.edu.cn*

‡Feng-Yuan Zhu and Xiaoli Zhang contributed to this work equally

Table of Contents

Chemicals and Materials

Nickel chloride hexahydrate ($NiCl_2 \cdot 6H_2O$, 98%) was purchased from Alfa Aesar. 2-Aminoterephthalic acid (H_2N-BDC), selenium powder (Se), melamine, and anhydrous ethanol were purchased from Tokyo Chemical Industry CO., Ltd. Pluronic F127 ($PEO_{100}PPO_{65}PEO_{100}$) was purchased from Shanghai Macklin Biochemical Co., Ltd. All reagents are used directly without further purification.

Material Characterization

The morphologies of the as-synthesized products were examined by scanning electron microscopy (SEM, Hitachi S-4700 and Regulus 8230) equipped with an energy dispersive X-ray spectrometer (EDS), transmission electron microscopy (TEM, TecnaiG220, FEI), and high-resolution TEM (HRTEM, Tecnai G2 F20 S-TWIN). X-ray diffraction (XRD) was performed on an X'Pert-Pro MPD diffractometer (Netherlands PANalytical) with a Cu Kα X-ray source (λ = 1.540598 Å). The ordering of carbon was tested by Raman spectroscopy (LabRam HR800, Horiba) with a 633 nm laser. X-ray photoelectron spectroscopy (XPS, Escalab250Xi, UK) was conducted with a hemispherical electron energy analyser. The specific surface area and pore size distribution were collected using the Brunauer-Emmett-Teller (BET, Micromeritics ASAP 2020 M) and Barrett-Joyner-Halenda (BJH) methods. Thermogravimetric analysis was performed using a TGA/DTA 6300 microanalyzer, and the sample was heated under a nitrogen stream of 100 mL min^{-1} with a heating rate of 10 °C min^{-1}.

Electrochemical Measurement

All electrochemical measurements were performed on a CS310 electrochemical workstation using a three-electrode setup at room temperature. A glass carbon (GC) disk electrode (5 mm in diameter), platinum electrode, and Ag/AgCl (KCl saturated) electrode were used as the working, counter and reference electrodes, respectively. Herein, 5 mg nanomaterials, 5 mg carbon powder, and 30 μL 0.5 wt% Nafion solution were dispersed in 0.97 mL isopropanol solution via an ultrasonic reaction for 1 h to form a catalyst slurry. Then, 21 μL of the above solution was dropped on the GC electrode and dried at room temperature. All potential values were referenced to a reversible hydrogen electrode (RHE): ERHE = $E_{Ag/AgCl}$ + 0.197 + 0.059 × pH. Linear sweep voltammetry (LSV) was measured in a 1 M KOH solution at a scan rate of 10 mV s^{-1}. All LSV curves were recorded with 95 IR correction. Chronopotentiometry (Cp) measurements were carried out on nickel foam (0.5 × 0.5 cm^2, loading 0.8 mg cm^{-2}). The electrochemically active surface areas (ECSAs) were estimated from the electrochemical double-layer capacitance (C_{dl}). The C_{dl} value was determined from cyclic voltammograms (CV) measured in a nonfaradaic region at different scan rates (v = 10, 20, 30, 40 and 50 mV s^{-1}) in the potential range -0.22 to -0.1 V versus Ag/AgCl. Electrochemical impedance spectrum (EIS) experiments were performed with a three-electrode cell system in 1 M KOH. The amplitude of the sinusoidal wave was 5 mV, and the frequency scan range was from 10^{-2} Hz to 10^5 Hz.

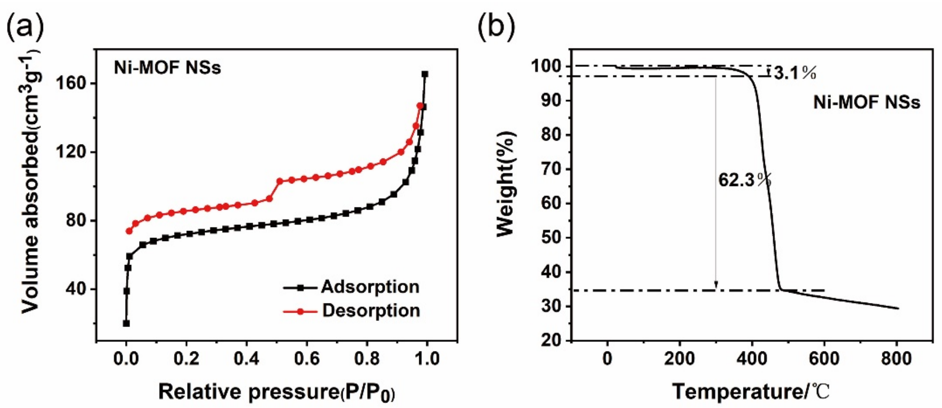

Fig. S1 (a) Nitrogen adsorption/desorption isotherms, and (b) thermogravimetric analysis plot of Ni-MOF NSs.

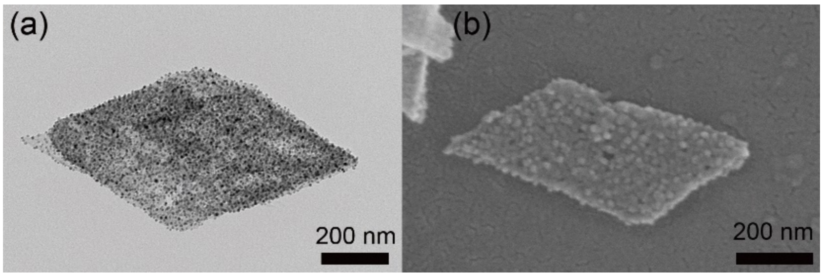

Fig. S2 (a) TEM, and (b) SEM of Ni-NPs/Ni-MOF NSs.

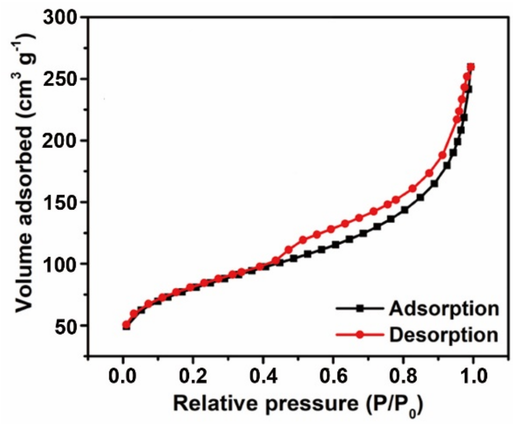

Fig. S3 Nitrogen adsorption/desorption isotherms of Ni-NPs/CNTs/Ni-MOF NSs.

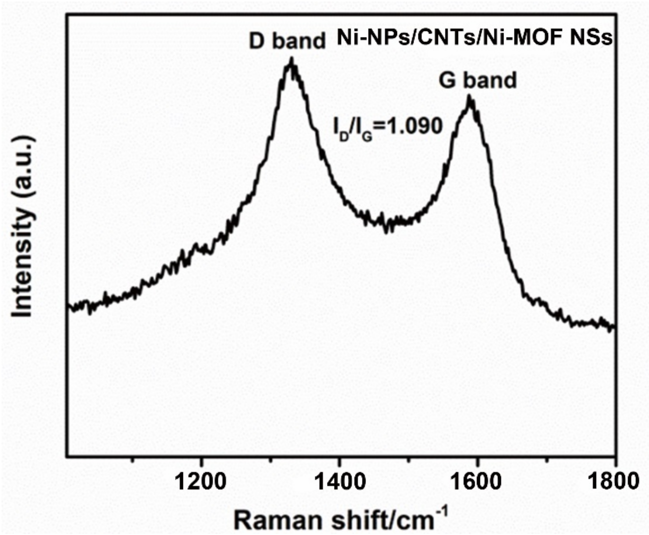

Fig. S4 The Raman spectra of Ni-NPs/CNTs/Ni-MOF NSs.

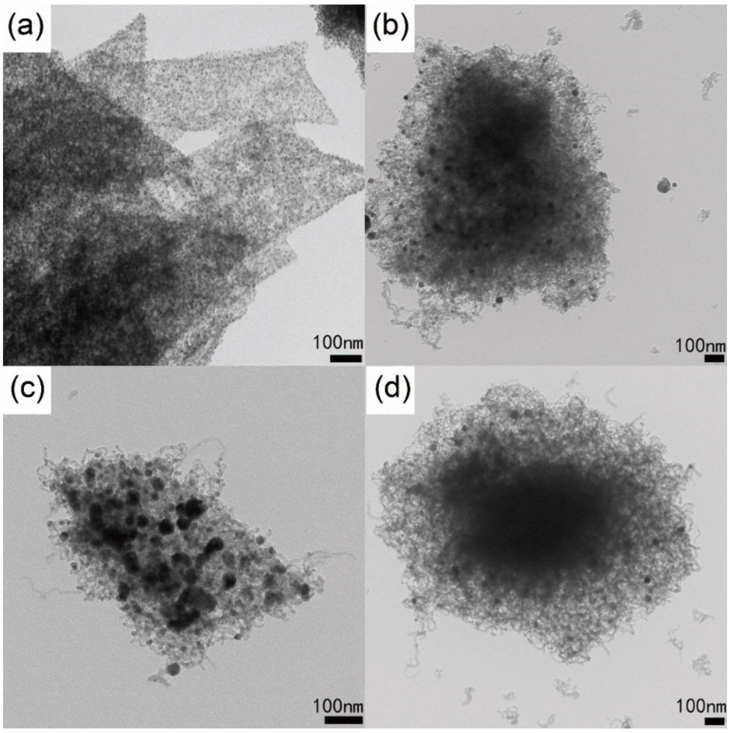

Fig. S5 TEM images of (a) Ni-NPs/CNTs/Ni-MOF NSs-400, (b) Ni-NPs/CNTs/Ni-MOF NSs-600, (c) Ni-NPs/CNTs/Ni-MOF NSs-700, (d) Ni-NPs/CNTs/Ni-MOF NSs-800.

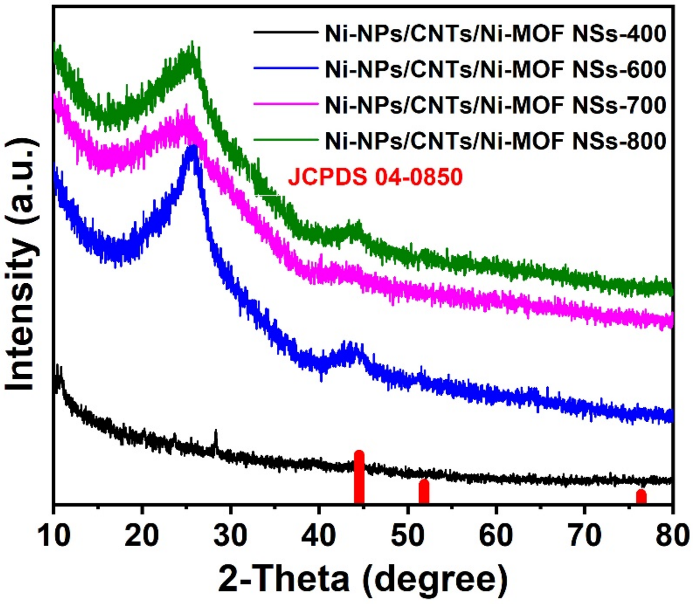

Fig. S6 PXRD patterns of Ni-NPs/CNTs/Ni-MOF NSs-400, Ni-NPs/CNTs/Ni-MOF NSs-600, Ni-NPs/CNTs/Ni-MOF NSs-700 and Ni-NPs/CNTs/Ni-MOF NSs-800.

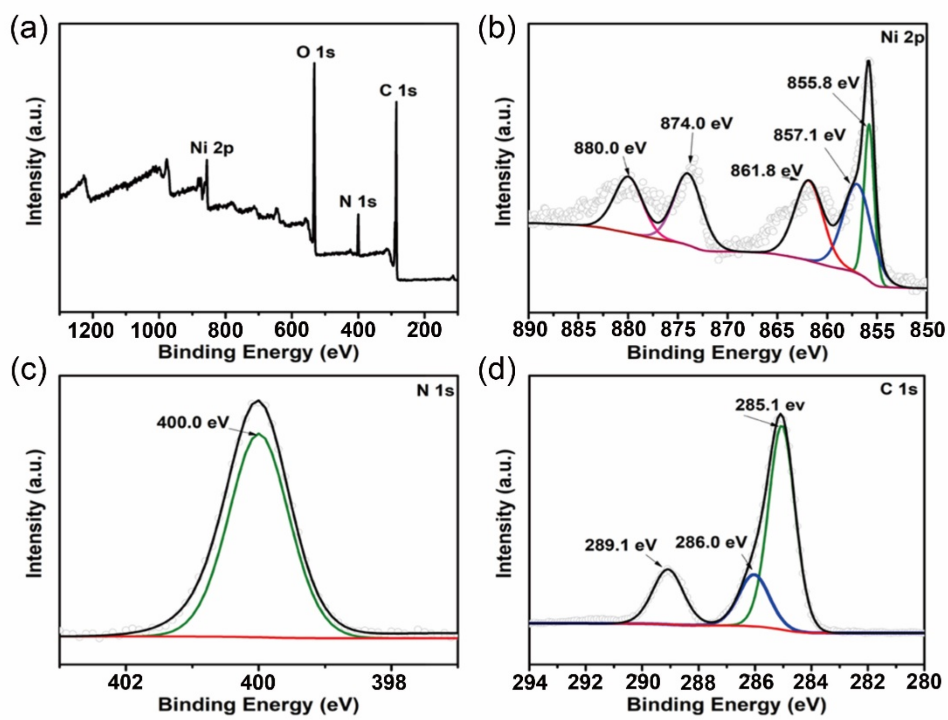

Fig. S7 (a) XPS survey spectrum, (b) Ni 2p XPS, (c) N 1s XPS and (d) C 1s XPS spectra of Ni-MOF NSs.

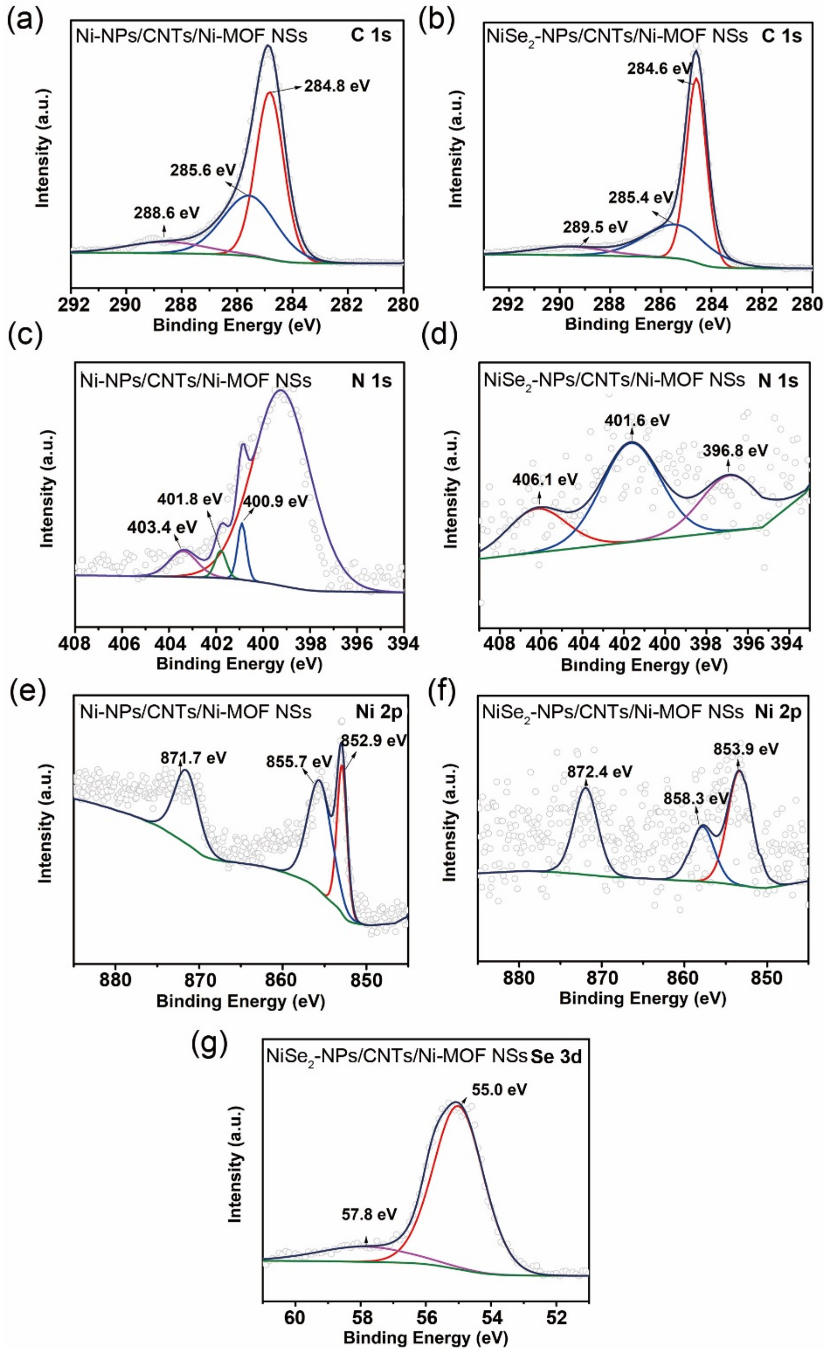

Fig. S8 (a) C 1s XPS, (c) N 1s XPS and (e) Ni 2p XPS spectra of Ni-NPs/CNTs/Ni-MOF NSs; (b) C 1s XPS, (d) N 1s XPS, (f) Ni 2p XPS and (g) Se 3d XPS of $NiSe_2$-NPs/CNTs/Ni-MOF NSs.

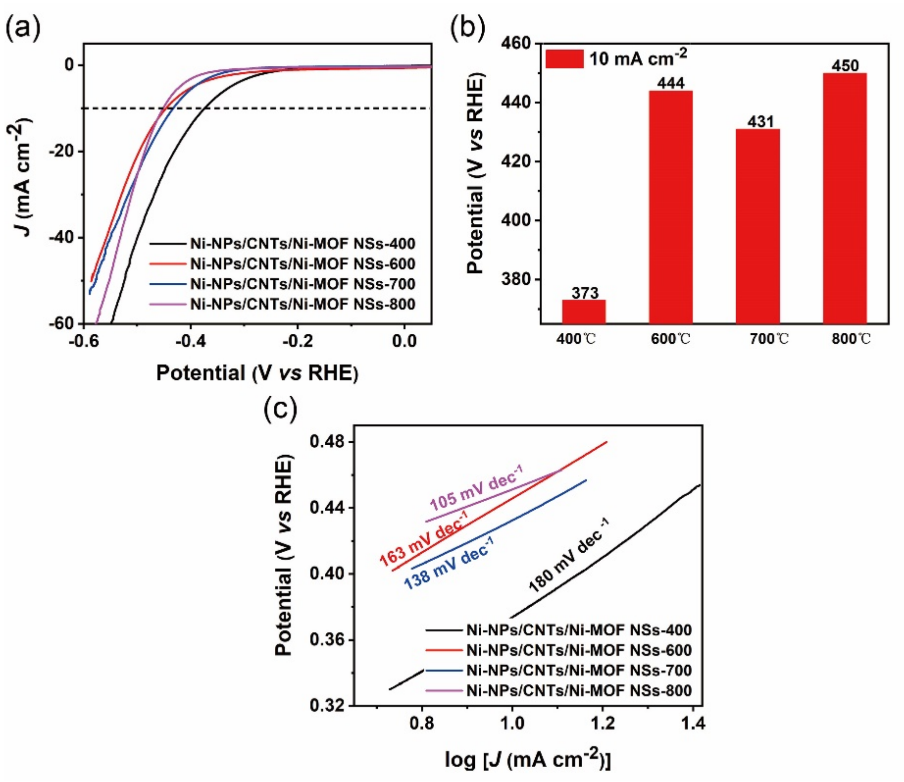

Fig. S9 (a) HER polarization curves of Ni-NPs/CNTs/Ni-MOF NSs-400, Ni-NPs/CNTs/Ni-MOF NSs-600, Ni-NPs/CNTs/Ni-MOF NSs-700, and Ni-NPs/CNTs/Ni-MOF NSs-800 in a 1 M KOH electrolyte. (b) The corresponding overpotentials at 10 mA cm^{-2}. (c) Tafel plots of different catalysts.

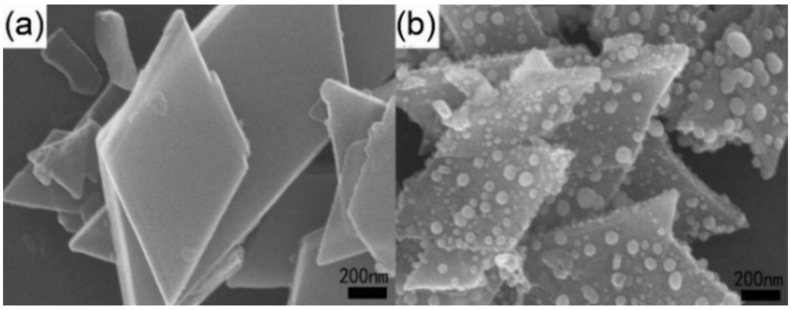

Fig. S10 SEM images of (a) Ni-MOF NSs and (b) Ni-NPs/Ni-MOF NSs after selenization.

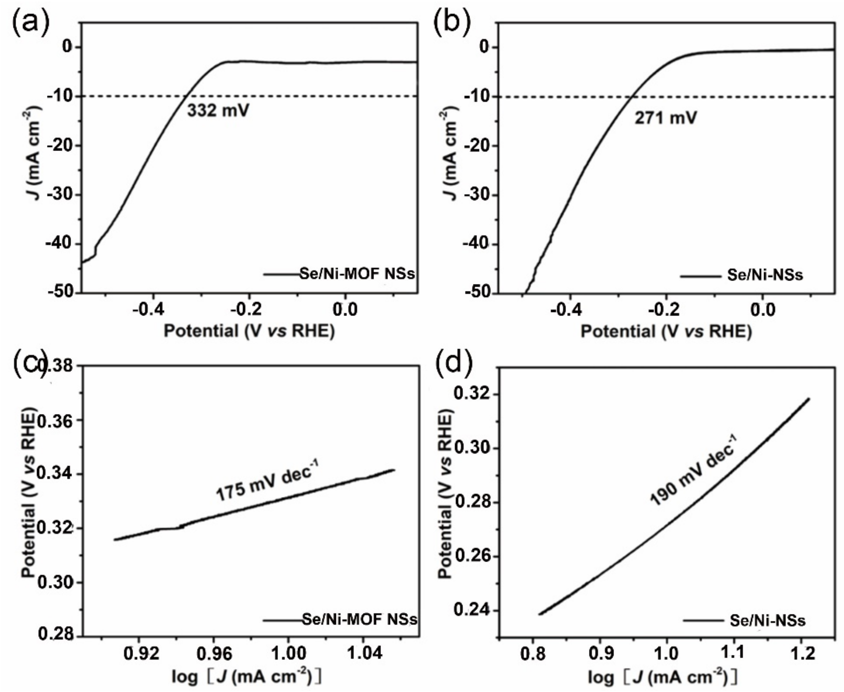

Fig. S11 HER polarization curves of (a) Ni-MOF NSs and (b) Ni-NPs/Ni-MOF NSs after selenization in a 1 M KOH electrolyte. Tafel plots of (c)Ni-MOF NSs and (d) Ni-NPs/Ni-MOF NSs after selenization.

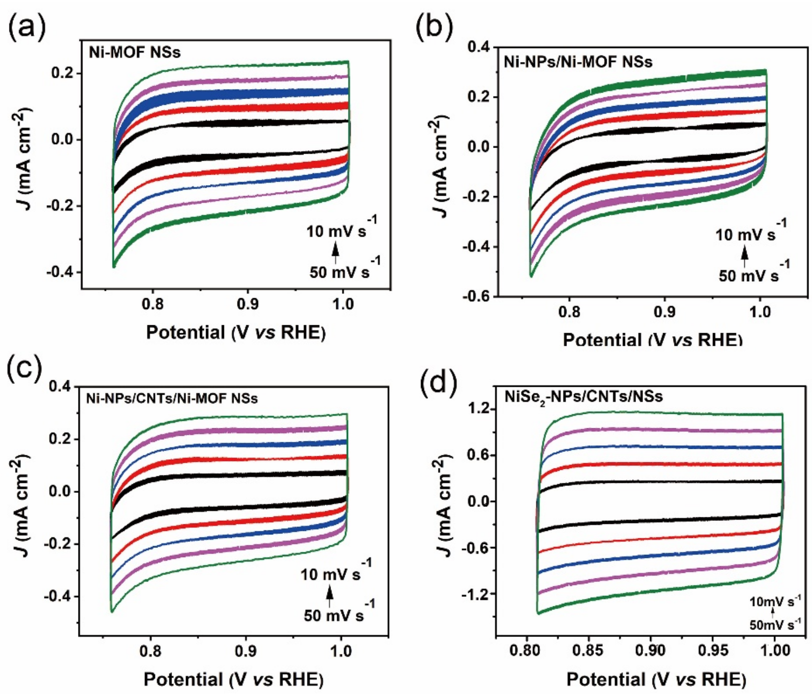

Fig. S12 CV curves of (a) Ni-MOF NSs, (b) Ni-NPs/Ni-MOF NSs, (c) Ni-NPs/CNTs/Ni-MOF NSs and (d) $NiSe_2$-NPs/CNTs/Ni-MOF NSs with different scan rates from 10 to 50 mV s^{-1}.

Table S1 The atomic ratio of C/N/Se/Ni from EDS analysis on $NiSe_2$-NPs/CNTs/Ni-MOF NSs.

Element	Wt %	At %
C K	72.81	90.19
N K	5.27	5.61
Se L	20.83	3.93
Ni K	1.09	0.27
Total	100.00	100.00

Table S2 Comparison of the HER performance of $NiSe_2$-NPs/CNTs/Ni-MOF NSs with the known HER electrocatalysts.

Number	Catalyst	η(10 mA cm^{-2})	Electrolyte	Reference
1	$NiSe_2$-NPs/CNTs/Ni-MOF NSs	165 mV	1.0 M KOH	This work
2	NiFeP@N-CS	186 mV	1.0 M KOH	[1]
3	$Ni_{90}P_{10}$	234 mV	1.0 M KOH	[2]
4	Ni_2P@mesoG	188 mV	1.0 M KOH	[3]
5	Ni_3Se_4	203 mV	1.0 M KOH	[4]
6	$NiSe_2$ NSs	184 mV	1.0 M KOH	[5]
7	$NiSe_2$@nitrogen-doped graphene	248 mV	1.0 M KOH	[6]
8	MoS_2-NiS_2/NGF	172 mV	1.0 M KOH	[7]
9	selenized Ni-Fe foam	181 mV	1.0 M KOH	[8]
10	Fe, Al-$NiSe_2$/rGO	197 mV	0.5 M H_2SO_4	[9]
11	$NiSe_2$ NSs	198 mV	0.5 M H_2SO_4	[10]
12	$NiSe_2$ and $Ni_{0.95}Se$ supported on nickel foam	175 mV	1.0 M KOH	[11]

References

(1) J. Hei, G. Xu, B. Wei, L. Zhang, H. Ding and D. Liu, *Appl. Surf. Sci.*, 2021, **549**, 149297.

(2) Q. Liu, C. Tang, S. Lu, Z. Zou, S. Gu, Y. Zhang and C. M. Li, *Chem. Commun.*, 2018, **54**, 12408-12411.

(3) S. Jeoung, B. Seo, J. M. Hwang, S. H. Joo and H. R. Moon, *Mater. Chem. Front.*, 2017, **1**, 973-978.

(4) S. Anantharaj, J. Kennedy and S. Kundu, *ACS Appl. Mater. Interfaces*, 2017, **9**, 8714-8728.
(5) H. Liang, L. Li, F. Meng, L. Dang, J. Zhuo, A. Forticaux, Z. Wang and S. Jin, *Chem. Mater.* 2015, **27**, 5702-5711.
(6) W. Li, B. Yu, Y. Hu, X. Wang, D. Yang and Y. Chen, *ACS Sustain. Chem. Eng.*, 2019, **7**, 4351-4359.
(7) P. Kuang, M. He, H. Zou, J. Yu and K. Fan, *Appl. Catal. B Environ.*, 2019, **254**, 15-25
(8) C. Zhang, Y. Bai, Y. Zhang, C. Li and S. Zhou, *Results Phys.*, 2019, **14**, 102522.
(9) L. Chen, H. Jang, M. G. Kim, Q. Qin, X. Liu and J. Cho, Fe, *Nanoscale*, 2020, **12**, 13680-13687.
(10) K. S. Bhat and H. S. Nagaraja, *Int. J. Hydrogen Energ*, 2018, **43**, 19851-19863.
(11) P. Ramakrishnan, S. Jo, N. Pitipuech and J. I. Sohn, *Electrochim. Acta.*, 2020, **354**, 136742.